Pergamon

Journal of Structural Geology, Vol. 20, No. 9/10, pp. 1325 to 1343, 1998

PII: S0191-8141(98)00082-0

0191-8141/98/ $ - see front matter

Exploding xenoliths and the absence of 'elephants' graveyards' in granite batholiths

D. BARRIE CLARKE, ANDREW S. HENRY

Department of Earth Sciences, Dalhousie University, Halifax, Nova Scotia, Canada B3H 3J5

and

MARY ANNE WHITE

Department of Chemistry, Dalhousie University, Halifax, Nova Scotia, Canada B3H 4J3

(*Received* 1 *July* 1997; *accepted in revised form* 20 *April* 1998)

Abstract—Biotite monzogranite near the eastern margin of the late Devonian South Mountain Batholith at Portuguese Cove, Nova Scotia, surrounds a large (20 m × 25 m), anisotropic (decimetre-scale interbedded psammite and semipelite) xenolith of the metamorphic (regional greenschist/thermal cordierite hornfels) country rocks of the Cambro-Ordovician Meguma Group. The xenolith has two distinct types of surfaces against the monzogranite: (i) one rounded, diffuse, and apparently old surface that had prolonged contact with the granite magma; and (ii) two straight, sharp, and apparently new surfaces that had more recently come into contact with the granite magma. More than 375 thin sheets (width < 0.1 cm, $n = 224$; 0.1–0.5 cm, $n = 66$; 0.5–1.0 cm, $n = 51$; 1.0–5.0 cm, $n = 30$; 5.0–10.0 cm, $n = 3$; > 10 cm, $n = 2$), ranging in composition from monzogranite to pegmatite to coarse quartz–sericite, cut the xenolith parallel to bedding producing a cumulative volume expansion of ~14% in the xenolith. Aspect ratios in some of the thin sheets exceed 1000:1. Several sheets cut the xenolith perpendicular to bedding producing a volume expansion of < 4%. We postulate that this pattern of sheet injection occurred in response to cracking of the xenolith by thermal stress fracturing following its incorporation into the granitic magma. Thermal modelling shows that stresses are highest in the pelite layers perpendicular to bedding leading to fracture parallel to bedding. We also consider that stored elastic strain energy and release of free aqueous vapour at the tips of propagating fractures may contribute to the disintegration of the xenolith. If explosive disintegration of large, anisotropic, passively stoped blocks of country rock is common, then this process may explain the absence of elephants' graveyards (accumulations of large stoped blocks) on the floors of granite batholiths, and high degrees of country rock contamination in some granite batholiths. © 1998 Elsevier Science Ltd. All rights reserved

INTRODUCTION

Daly (1903a,b, 1933) formalized the process of blocks of country rocks sinking from the roof of a pluton into a magma as 'stoping', and stoping has since become recognized as one of the classic mechanisms of emplacement of granitic magmas. The principal line of evidence for such a process is the common occurrence of blocks of country rock in the marginal facies of granitoid intrusions. That stoping occurs on *some* scale is generally accepted (Goodchild, 1892, 1894; Daly, 1903a, 1933; Balk, 1937; Read, 1948; Buddington, 1959; Marsh, 1982; Castro, 1987; Clemens and Mawer, 1992; Pitcher, 1993; Paterson *et al.*, 1996), but three major questions remain: (i) what is the mechanism by which blocks of country rock become dislodged from the roofs of plutons?; (ii) given that emplacement upwards is equivalent to ascent, what proportion of the total ascent of a granite magma can stoping account for?; and (iii) what is the ultimate fate of the stoped blocks? The third question, concerning the fate of the stoped blocks, is the subject of this paper, and finding an answer to it will also provide insight into the second one.

In part, the problem of stoping is one of scale. Should granite batholiths, with dimensions measured in tens to hundreds of kilometres, dislodge roof blocks having dimensions measured in centimetres or metres (the common sizes of xenolithic fragments in granites)? More likely, the original stoped blocks were tens to hundreds of metres in size, yet if this were the case, and if the large xenoliths remained intact during descent through the magma chamber, the stoping process should produce an accumulation zone at the bottom of the batholith consisting of variably dimensioned, stratigraphically jumbled, and structurally misaligned blocks, surrounded by granite. Such zones, informally termed 'elphants' graveyards', are essentially unknown, and this apparent absence has often been held as evidence against the mechanism of stoping itself (Buddington, 1959).

That argument is flawed in several respects. For one, the absence of evidence for elephants' graveyards is not necessarily evidence for absence of stoping because we may be wrong in our concept of such a zone. Such an argument is based on the assumption that the stoped blocks maintain their physical integrity after dropping from the roof toward the floor of the magma chamber. This paper is a preliminary examination of the physical state of one stoped block in the South Mountain batholith, and its consequences for both elephants' graveyards and the assimilation–contamination model.

REGIONAL GEOLOGY AND FIELD OBSERVATIONS

The Meguma Zone is the most outboard lithotectonic terrane in the Appalachian system (Williams and Hatcher, 1982), and consists of two principal rock types (Fig. 1). The Cambro-Ordovician Meguma Group is a proximal and distal flyschoid turbidite sequence with well-developed Bouma sequences (Schenk, 1991). The Acadian orogenic event (410–390 Ma) deformed the Meguma Group into isoclinal folds, and regionally metamorphosed it to greenschist facies in south-central Nova Scotia. Intruding the Meguma Group is the South Mountain batholith (SMB), a large, late-Devonian, syntectonic (Benn *et al.*, 1997) to post-tectonic, intrusive complex consisting of peraluminous granitoid rocks ranging in composition from granodiorite to leucogranite (Clarke and Muecke, 1985; MacDonald *et al.*, 1992; Clarke *et al.*, 1993).

The eastern contact of the SMB at Portuguese Cove consists dominantly of magmatic flow-foliated biotite monzogranite containing abundant aligned K-feldspar 'dents-de-cheval' up to 10 cm long (MacDonald and Horne, 1987, 1988; Abbott, 1989). The foliated biotite monzogranite is cut by late-stage aplite, aplite–pegmatite, and pegmatite dykes with sharply defined contacts.

Tate (1994) noted that the endocontact region of the South Mountain Batholith contains abundant ellipsoidal decimetric xenoliths of the country rock. One xenolith at Portuguese Cove is unique (Cooke and Milligan, 1980). It is roughly triangular in plan, has maximum dimensions of 20×25 m, and is apparently completely surrounded by granitoid rocks (Fig. 2). As observed elsewhere (Fowler and Paterson, 1997), regional foliation trends in the biotite monzogranite change their orientation only near the xenolith, and also non-foliated coarse-grained granitoid material occurs in the vicinity of the xenolith. The xenolith itself consists of typical Meguma Group rock types, composed of easily distinguished interbedded wackes and mudstones, regionally metamorphosed to greenschist facies, and then subsequently thermally metamorphosed to cordierite hornfels facies. What sets this xenolith apart from country rocks in the thermal aureole of the SMB is its coarse sericite and complete pinitization of the cordierites. The orientation of the bedding in the xenolith is reasonably consistent with that of *in situ* country rocks nearby.

The most remarkable aspect of this xenolith is the extent to which it is fractured. In detail, it shows the following macroscopic features:

(i) *Types of bounding surface* (Fig. 3 a–c)—The xenolith has three distinct types of surface against the biotite monzogranite: (a) the rounded, diffuse, and relatively old northeastern surface that appears to

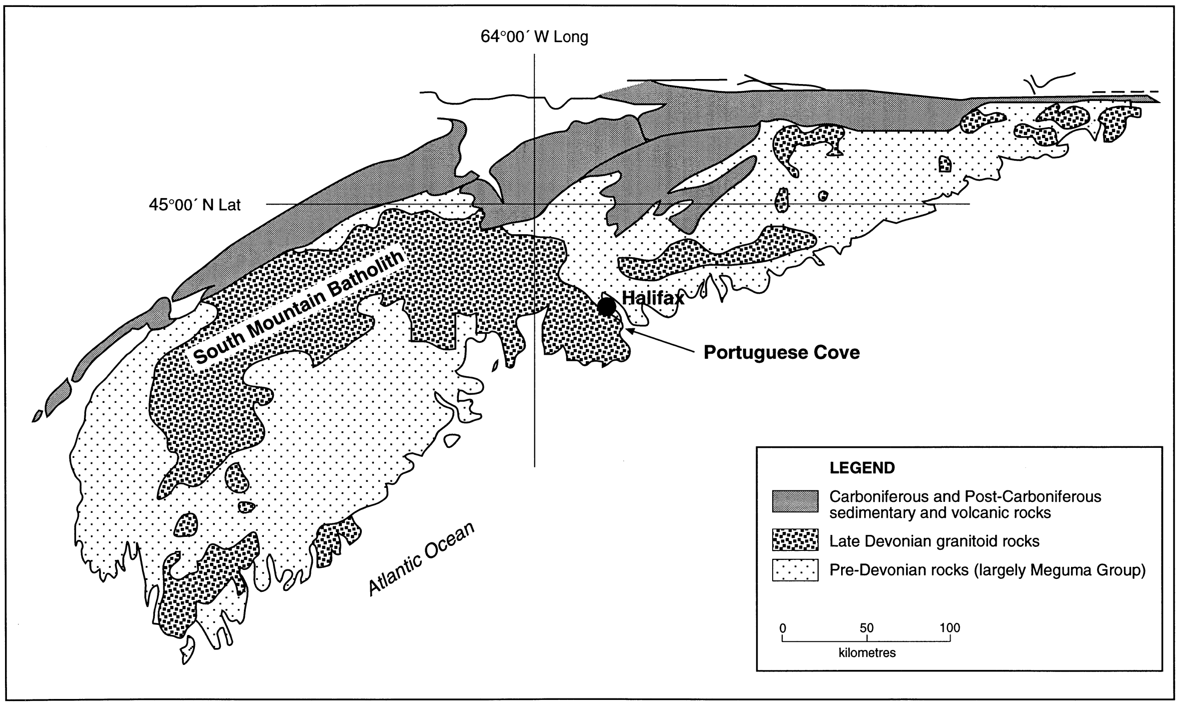

Fig. 1. Location map of southern Nova Scotia showing the South Mountain Batholith and the position of Portuguese Cove near its eastern contact with the Meguma Group.

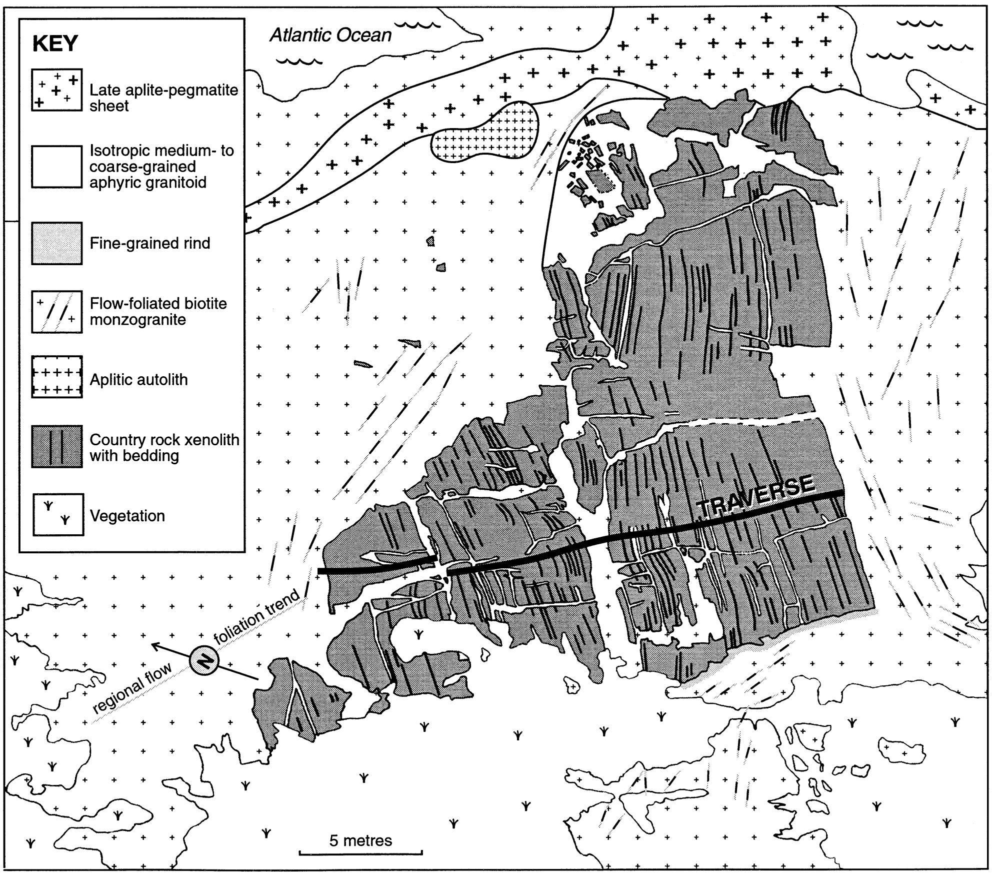

Fig. 2. Map of the large xenolith at Portuguese Cove. Principal features include the disruption of the regional flow foliation in the biotite monzogranite in the vicinity of the xenolith, the occurrence of a fine-grained granitoid rind at the west end of the xenolith, a medium- to coarse-grained aphyric granitoid at the east end, and the obvious fragmentation of the xenolith itself.

have had a prolonged contact with the granite magma; (b) the straight, sharp, and relatively new southern surface, parallel to the strike of bedding in the xenolith, that appears to have been in contact with the granite magma for only a relatively short time; and (c) the straight, sharp, western surface perpendicular to strike of bedding in the xenolith that is apparently also a relatively new surface that appears to have been in contact with the granite magma for only a relatively short time, but this surface has a distinct finer-grained (aplitic?) rind 0.25 m thick (under the scale in Fig. 3c).

(ii) *Fracture pattern in the xenolith* (Fig. 4)—More than 375 thin sheets (width <0.1 cm, $n = 224$; 0.1–0.5 cm, $n = 66$; 0.5–1.0 cm, $n = 51$; 1.0–5.0 cm, $n = 30$; 5.0–10.0 cm, $n = 3$; >10 cm, $n = 2$), ranging in composition from monzogranite to aplite–pegmatite to relatively coarse quartz–sericite, cut the xenolith parallel to bedding producing a cumulative volume expansion of ~14% in the xenolith. Aspect ratios in some of the thin sheets exceed 1000:1. Several minor sheets cut the xenolith perpendicular to bedding producing a volume expansion of $<4\%$ in that direction.

(iii) *Tapered intrusive sheets* (Fig. 5a & b)—Many of the bedding-parallel intrusive sheets are not uniform in width, but rather taper down from west to east. The wider the sheet, the more likely it is to be typical porphyritic biotite monzogranite similar to the material enclosing the xenolith. The thinner the sheets are, the more likely they are to be aplite–pegmatite, pegmatite alone, or just coarse quartz–sericite (see later). Judging from the direction of taper of the granitic sheets, the western margin of the xenolith is also the magma intake surface. Significantly, it is the only apparently younger surface of the xenolith perpendicular to bedding.

(iv) *Ductily deformed eastern margin* (Fig. 5c)—At the eastern end of the xenolith, several partially dislodged pieces of the main xenolith show distinct folding.

(v) *Distribution of satellite xenolithic fragments* (Fig. 5d)—The monzogranite host along the northeastern and eastern sides of the xenolith contains dozens of sharply angular xenolithic fragments, many of which fit together in jigsaw-like fashion. Some groups of xenoliths resemble a deck of playing cards jettisoned into the magma.

PETROGRAPHIC DESCRIPTIONS

Granitoid material outside the xenolith

Figure 6 illustrates the four distinctly different textural types of granitoid rock that surround the large xenolith. The foliated biotite monzogranite that generally characterizes this area (Fig. 6a) is different from the isotropic, leucocratic, equigranular, medium- to coarse-grained, granitoid material at the eastern contact of the large xenolith (Fig. 6b). Also, the typical late aplites (Fig. 6c) that occur throughout the region are different from the fine-grained rind on the western contact (Fig. 6d). We believe that these textural variations are significant in terms of the processes that were occurring in the vicinity of the xenolith at the time of its incorporation into the magma.

Granitoid material inside the xenolith

Figure 7 illustrates several textural features of the granitoid material inside the fractures in the large xenolith:

(i) *Normal hypidiomorphic granular granitoid texture*—In some wide fractures, the texture of the granitic material is generally indistinguishable from the biotite monzogranite outside the xenolith (Fig. 7a).

(ii) *Quartz in a matrix of feldspar and muscovite*—Many of the fracture-fills have modal mineralogical compositions that are quartz-rich relative to common granitoid rocks, and in these sheets the feldspar and muscovite form an interstitial matrix around the quartz grains (Fig. 7b).

a

b

Fig. 3 (a & b)—*Caption opposite*.

c

Fig. 3. Contrasting surfaces on the xenolith. (a) Diffuse, irregular, old northeastern contact is just above the scale. (b) Razor sharp, linear, strike-parallel, new southern contact surface. Note abundant granitoid-filled fractures in the xenolith and 'dents-de-cheval' in the biotite monzogranite. (c) Razor sharp, linear, strike-perpendicular, new western contact surface. Note abundant granitoid-filled fractures in the xenolith, fine-grained rind, and cluster of K-feldspar phenocrysts in the foliated biotite monzogranite. Scale is 25 cm long.

(iii) *Comb textures and quartz–feldspar intergrowth*—In some samples, the quartz–feldspar boundaries show a high degree of sinuosity, and even comb textures, suggesting that the two mineral phases are not in textural equilibrium. An extension of this textural relationship is a quartz–feldspar laminar intergrowth (Fig. 7c).

(iv) *Millimetre-scale aplite–pegmatite development*—On close inspection, many of the mm-scale fracture fillings consist of miniature 'aplite–pegmatite' systems, with fine-grained margins and coarser cores in which the grain sizes are an order of magnitude larger than those at the margins (Fig. 7d).

(v) *Euhedral cordierites*—The euhedral cordierite (probably magmatic; Fig. 7e) pseudomorphs in the fractures are distinct from the oval cordierite (probably thermal metamorphic) pseudomorphs in the country rock.

(vi) *Fracture-parallel andalusites*—One of the most unusual textures consists of elongate quartz grains poikilitically enclosing andalusites aligned parallel to the margins of the distal ends of fractures (Fig. 7f). The parallel extinction of all andalusites suggests that they may be parts of a single skeletal andalusite, and not individual grains.

The macroscopic features, particularly the number of intrusive sheets, their tapered shapes, and the distribution of satellitic xenoliths, suggest a sudden, and perhaps violent, intrusive event, rather than a slow and passive invasion of the xenolith along bedding and cleavage planes (in this case, what would be the driving force?). Most of these microscopic textures are not typical of the hypidiomorphic granular textures developed in slowly crystallized granitic magmas. In addition, the radial clusters or sprays of muscovite which characterize so many of the fracture-fills suggest rapid crystallization. We interpret this collection of unusual textural features as the product of extremely fast disequilibrium crystallization in rapidly propagated fractures. The perthitic textures in some K-feldspars, however, indicate slow cooling; therefore, the rapid disequilibrium crystallization is likely to be the product of pressure quenching, not thermal quenching.

DISCUSSION

We offer as a working hypothesis that the country rock xenolith has shattered (literally exploded), and that the intrusive material cutting it ranges from true monzogranite at the intake, or proximal, end, through something resembling miniature aplite–pegmatite dykes, to discontinuous (in two dimensions), quartz–sericite veins, and finally to coarsely recrystallized muscovite at the distal end. In this section, we address questions concerning the stoping and block disintegration processes.

Causes of intense fracturing/fragmentation/disintegration/spalling

Grady and Kipp (1985) identified inherent flaws, available energy for fracturing, and strain rate as the principal factors governing fragment size during disintegration of a material. However, "no scientifically justified and physically consistent fragmentation model" exists to describe the mechanisms of fracture and sizes

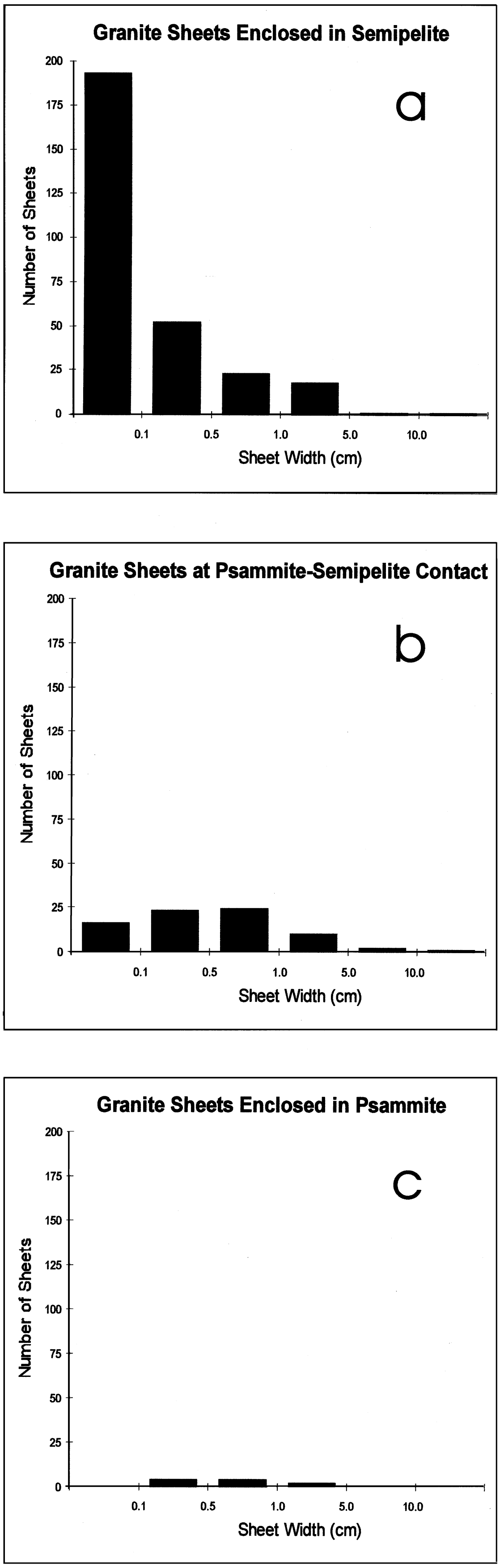

Fig. 4.

of particles produced during fragmentation (Ivanov *et al.*, 1995). Even so, we can explore quantitatively and qualitatively three factors that probably contributed to the disintegration of the large xenolith at Portuguese Cove.

Thermal stresses. The effects of heat to produce spallation are well known in nature as in calving of icebergs and sea ice, exfoliation of rocks, and disintegration of meteorites. These effects are also applied in flame-jet spallation drilling (Rauenzahn and Tester, 1989) and quarrying by fire (Marsh, 1982). Thermal stress fracturing results when thermally induced stresses exceed the rock strength. Sudden temperature increases in an isotropic substance can lead to thermal gradient cracking, whereas sudden temperature increases in an anisotropic substance can lead to thermal expansion anisotropy cracking or thermal expansion mismatch cracking, and possibly thermal gradient cracking. An analogous process for the fracturing of the large stoped block at Portuguese Cove may be the dropping of an ice-cube into a glass of water. Commonly, the ice-cube fractures with a loud cracking sound (the fracture propagation is extremely fast), and less commonly the thermal stress fracturing process is so intense that the ice-cube disintegrates into a number of small fragments. Temperature differences between the ice-cube and water are probably less than 20 K. We now show that temperature differences between the country rock and enclosing magma will produce stresses exceeding the strength of the country rock.

To understand thermally induced stresses originating from hot magma coming into contact with country rock, we have modelled this system as follows. The heat transfer between hot magma and colder country rock was treated as a one-dimensional problem between two semi-infinite media, truncated only by their common boundary; as the resulting thermal gradients for these materials proved to be negligible beyond a few tens of metres from the interface, the semi-infinite postulate is reasonable. Carslaw and Jaeger (1959) developed solutions of this problem giving the evolution of the temperature as a function of time (t) and distance (d) from the interface, here written in terms of the temperature of the magma (T_m), the temperature of the country rock (T_c), the initial temperature of the magma (T_m^0), the original temperature of the country rock (T_c^0), the thermal conductivity of the magma and country rock (k_m and k_c, respectively), and the thermal diffusivity of the magma and the country rock (a_m and a_c, respectively):

Fig. 4. Statistical data on granitoid intrusions from traverse on Fig. 2. (a) Most fractures occur within the pelite horizons, and the fracture fillings are equal to, or less than, 0.1 cm in width. These statistics suggest exploitation of inherent weaknesses in the cleaved pelites. (b) A smaller number of fracture fillings occupy the psammite–pelite contacts. (c) In general, the more isotropic psammitic horizons resist fracturing.

$$T_{\mathrm{m}} = T_{\mathrm{c}}^{0} + \frac{k_{\mathrm{m}} a_{\mathrm{m}}^{-1/2}\left(T_{\mathrm{m}}^{0} - T_{\mathrm{c}}^{0}\right)}{k_{\mathrm{m}} a_{\mathrm{m}}^{-1/2} + k_{\mathrm{c}} a_{\mathrm{c}}^{-1/2}} \times \left(1 + \frac{k_{\mathrm{c}} a_{\mathrm{c}}^{-1/2}}{k_{\mathrm{m}} a_{\mathrm{m}}^{-1/2}} \operatorname{erf}\left(\frac{d}{2(a_{\mathrm{m}} t)^{1/2}}\right)\right) \quad (1)$$

and

$$T_{\mathrm{c}} = T_{\mathrm{c}}^{0} + \frac{k_{\mathrm{m}} a_{\mathrm{m}}^{-1/2}\left(T_{\mathrm{m}}^{0} - T_{\mathrm{c}}^{0}\right)}{k_{\mathrm{m}} a_{\mathrm{m}}^{-1/2} + k_{\mathrm{c}} a_{\mathrm{c}}^{-1/2}} \operatorname{erfc} \frac{d}{2(a_{\mathrm{s}} t)^{1/2}} \quad (2)$$

where erf is the error function:

$$\operatorname{erf}(x) = \frac{2}{\pi^{1/2}} \int_{t=0}^{t=x} \mathrm{e}^{-t^2}\, \mathrm{d}t \quad (3)$$

and erfc is its complement:

$$\operatorname{erfc}(x) = 1 - \operatorname{erf}(x). \quad (4)$$

By treating the magma as a solid, and limiting heat transfer to conduction, this model neglects convection within the magma. The temperature of the magma at the interface could remain constant, or even increase, as the stoped block falls into the magma, but these effects are neglected. Furthermore, the latent heat of crystallization of the magma is not included. As these three effects would add to the heat flux to the country rock, the present model can be considered to give a lower limit of the thermal stress in the country rock.

Following Daly's method (Daly, 1903a), the thermal expansion and the pressure required to prevent thermal expansion (i.e. the thermal stress) within the country rock were calculated as functions of time and distance from the interface. This calculation required knowledge of a variety of thermal properties of magma and country rock (both psammite and pelite), including those listed above as well as thermal expansivity (α_V $[=V^{-1}(\partial V/\partial T)_p]$ on the basis of volume, and α_i $[=i^{-1}(\partial i/\partial T)_p]$ based on the *i*-axis in the unit cell) and bulk modulus B $[=-V(\partial P/\partial V)_T]$. Table 1 summarizes the values of thermal parameters used here and their sources. Specifically, the relative increase in volume, $\Delta V/V$ resulting from thermal expansion is related to the applied pressure (thermal stress, ΔP) required to suppress the expansion as

$$\frac{\Delta V}{V} = \alpha_{\mathrm{v}} \Delta T = \frac{\Delta P}{B} \quad (5)$$

for an isotropic system (e.g. psammite) and for an anisotropic system (e.g. pelite), this relationship can be written as:

$$\frac{\Delta i}{i} = \alpha_{\mathrm{i}} \Delta T = \frac{\Delta P}{3B} \quad (6)$$

where $\Delta i/i$ is the relative increase in the i^{th} direction.

The purpose of this model calculation is to see how the thermal stress within the country rock compares with the rock strength. (We ignore any contribution of stresses already present in the system that would be released on fracture, lowering the rock strength.) For the purposes of this discussion, the rock strength is taken to be 2×10^8 Pa for psammite and for pelite (Clark, 1966). Although the pelite strength would be expected to be anisotropic, the effect appears to be slight. From Fig. 8, it can be seen that after 1 h of contact the thermal stress for psammite and for the *a*-axis (parallel to bedding) direction in pelite, within the assumptions of this model, is less than the rock strength. However, the thermal stress of pelite in the direction of the *c*-axis (perpendicular to bedding) exceeds the threshold for fracture. The main reason for this difference is the three-fold larger thermal expansivity of pelite in this direction compared with the basal plane, as one would expect based on weaker interactions between layers than within layers. Therefore, Daly's conclusion (Daly, 1933) that "the stresses produced by this differential heating can hardly fail to break and exfoliate the country rocks" requires some qualification, as at somewhat lower temperature differentials, some materials and some directions within the country rock could be more susceptible to failure than others. Thus, on the basis of this model, fracture should occur parallel to bedding, and should happen only a short time after magma and country rock come into contact. Fractures would be expected to occur primarily within the pelite layers, with fewer fractures in the psammite, as observed.

The present results can be compared with an earlier model (Furlong and Myers, 1985) in which a 3 km spherical magma body is treated as an intrusion in country rock. Theirs is also a time-dependent coupled thermal and mechanical model, and it shows stress in excess of rock strength after rather short times (e.g. 0.1 y) at short distances (e.g. 0.3 m) from the magma–country rock interface, but under more extreme temperature gradients (their initial temperature difference between magma and country rock is five times that used here). Our model extends the conclusions of Furlong and Myers to shorter times (10^{-4} y) and a smaller temperature differential, showing that fracture can take place very close to the interface even on this very short time scale in these less extreme conditions. Furthermore, by including inhomegeneity in the country rock in two ways—material type (psammite and pelite) and thermal anisotropy (in pelite)—we have shown that fracture is preferential in the pelite in the direction that separates the layers of its structure.

Once fractures begin, they reduce the energy of the system by releasing stress (and the present model shows that such a process would be favoured because the thermal stress exceeds the material strength), but they cost energy because of the increase in surface area and restructuring of the bonds in the region of the fracture. In this case, the fracturing would occur from west to east, predominantly along the pelitic horizons. Field observations confirm this result. There is further evidence (see below) that this fracture takes place in the presence of an aqueous fluid phase, which is well known for lowering the surface energy in the region of the crack (Michalske and Bunker, 1987), assisting crack propagation.

Stored elastic strain energy. The Portuguese Cove xenolith belonged to the Meguma Group which underwent deformation during the Acadian Orogeny. As in

a

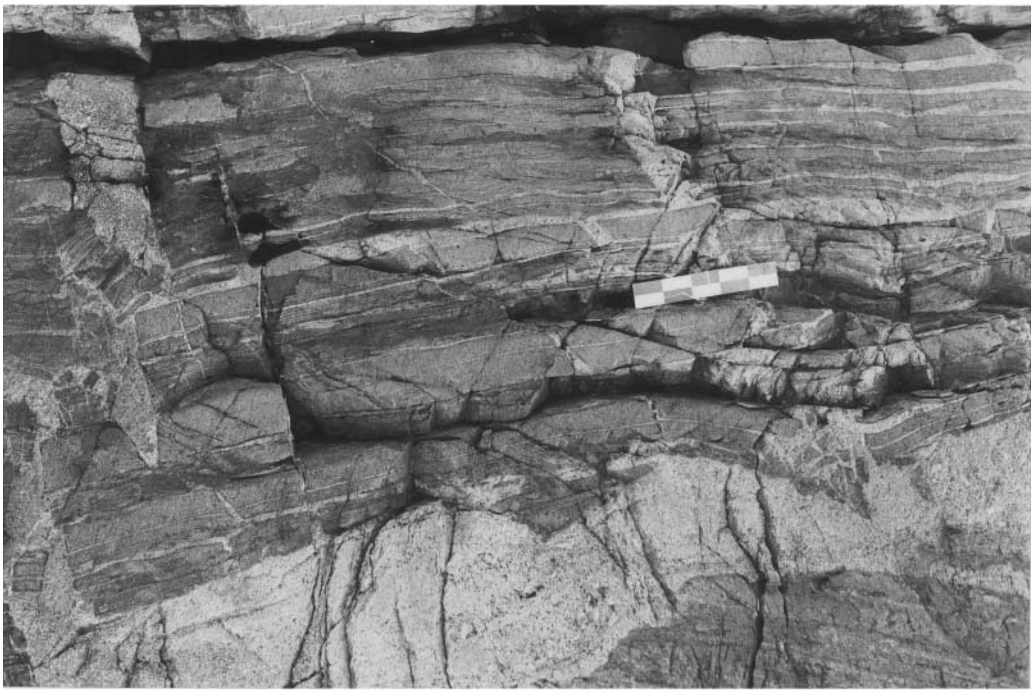

b

Fig. 5 (a & b)—*Caption opposite*.

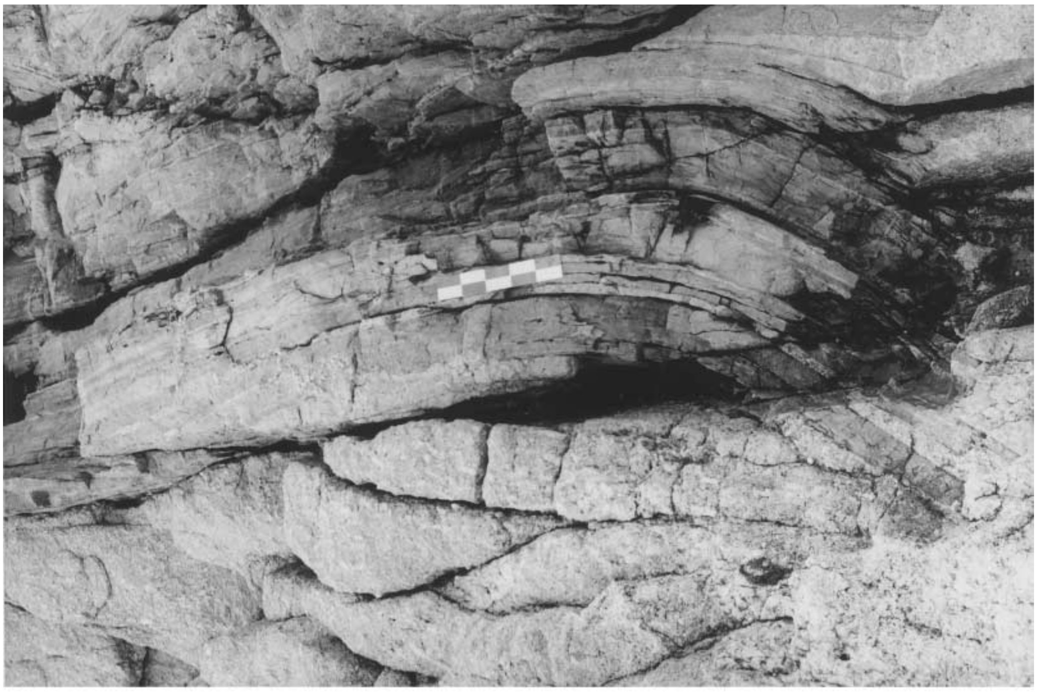

c

d

Fig. 5. Fracture and intrusive pattern in the xenolith. (a) Typical bedding-parallel fractures. Note that the central fracture tapers down significantly from the west (left) to the east (right). (b) Internal disintegration in the large spalled block on northeast side of the xenolith. Note how well the disaggregated pieces fit together. (c) Eastern margin of the large xenolith showing strong ductile deformation. (d) A collection of xenolithic shrapnel at the eastern contact set in a matrix of aphyric, medium- to coarse-grained granitoid. Note also the fragmentation of the fragments. Scale is 25 cm long.

the case of Rupert's drops (tear-drop shaped blobs of glass quenched in cold water, and having a high degree of stored elastic strain energy that can be released simply by breaking their tips), the country rock may also have contained some residual elastic strain energy. Its passage from an anisotropic stress environment as country rock to the isotropic environment of the granite magma as a stoped block may favour release of this energy. At this stage in our understanding of the xenolith, we can only note the possibility that stored elastic strain energy may have contributed to the rapid disintegration of the xenolith.

Aqueous vapour phase expansion. Lister and Kerr (1991) and Rubin (1993a, b, 1995) have shown that the tip of a crack being intruded by magma will contain an aqueous fluid phase. The fluid not only lowers the surface energy of the solid and helps to break

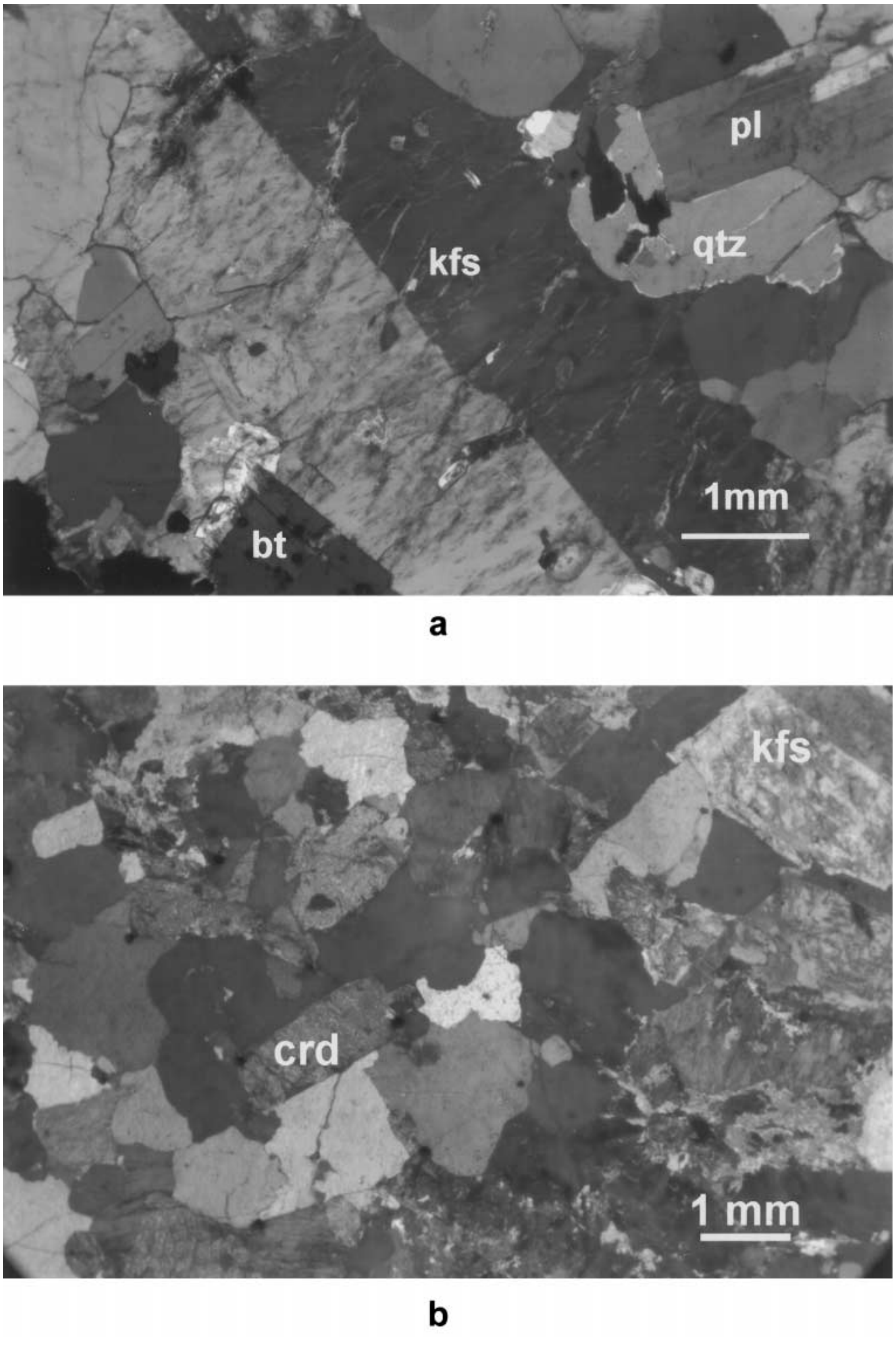

Fig. 6 (a & b)—*Caption opposite*.

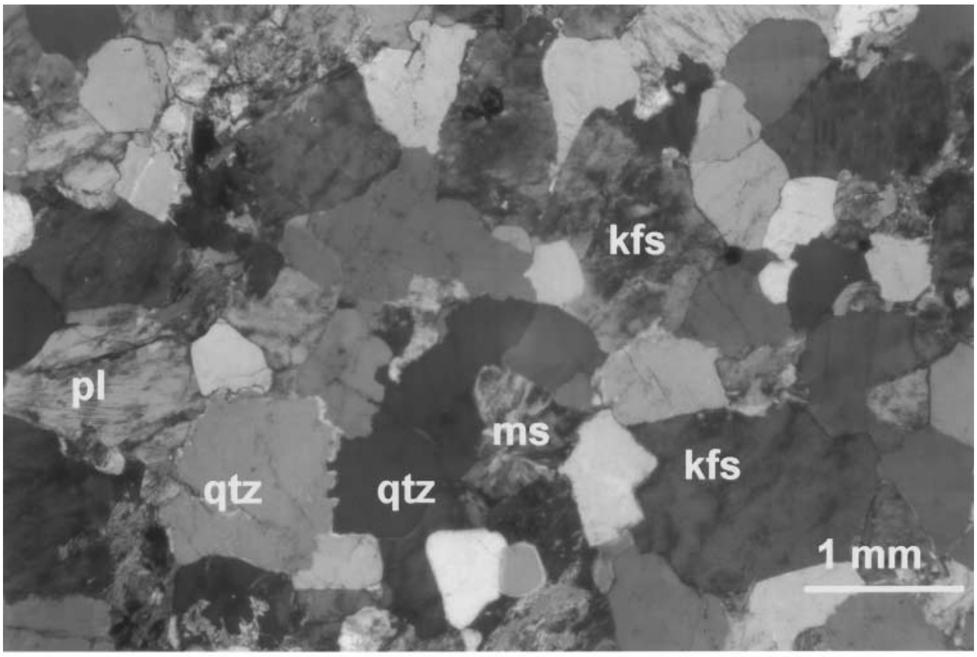

c

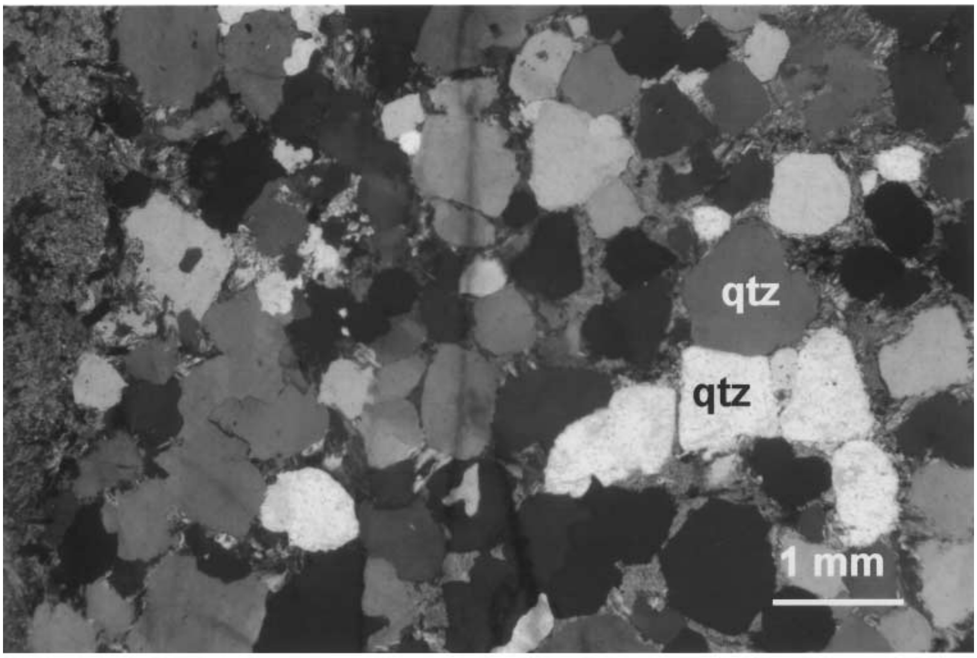

d

Fig. 6. Petrographic features of the granitoid rocks outside the fractured xenolith. (a) Sample PCX16b, a typical flow foliated regional biotite monzogranite with large 'dents-de-cheval' phenocrysts of potassium feldspar. (b) Sample PCX20, the cordierite-rich isotropic granitoid from the eastern end of the xenolith. (c) Sample PCX16 d, a late aphyric aplite dyke with characteristic interlocking texture among the grains. (d) Sample PCX7c, the fine-grained rind on the western end of the xenolith, an apparent mechanical collection of quartz grains in a continuous matrix of feldspar and muscovite.

bonds, but also promotes fracture propagation by volumetric expansion. If the vapour pressure is greater than the tensile strength, crack propagation will be rapid and internal fragmentation may occur. Depending on a wide range of variables, fracture propagation rates may range from $0.5\,\mathrm{m\ s^{-1}}$ for magma-driven propagation (Spence and Turcotte, 1985), to about half the Rayleigh wave velocity for kinetically induced fracturing (Glenn *et al.*, 1986).

The emergence and further(?) expansion of the fluid at the distal (eastern) end of the xenolith may have resulted in fragmentation of that surface and apparently violent dispersal of the xenolithic fragments, similar to that produced by the vaporization and fragmentation experiments that model erupting magmas (Sugioka and Bursik, 1995). In addition, the ductile deformation of fragments at the eastern end of the xenolith is similar to that produced in materials placed near the seat of an explosion (Tardif and Sterling, 1967). If our interpretation of an explosive event is correct, then the small angular satellitic xenoliths are best described as xenolithic 'shrapnel'. Daly (1933, p. 275) had a similar view of the explosive nature of the stoping process itself when he stated that "...the shell of country rocks becomes packed with tensions. These surely accumulate until the shell 'flies to pieces'".

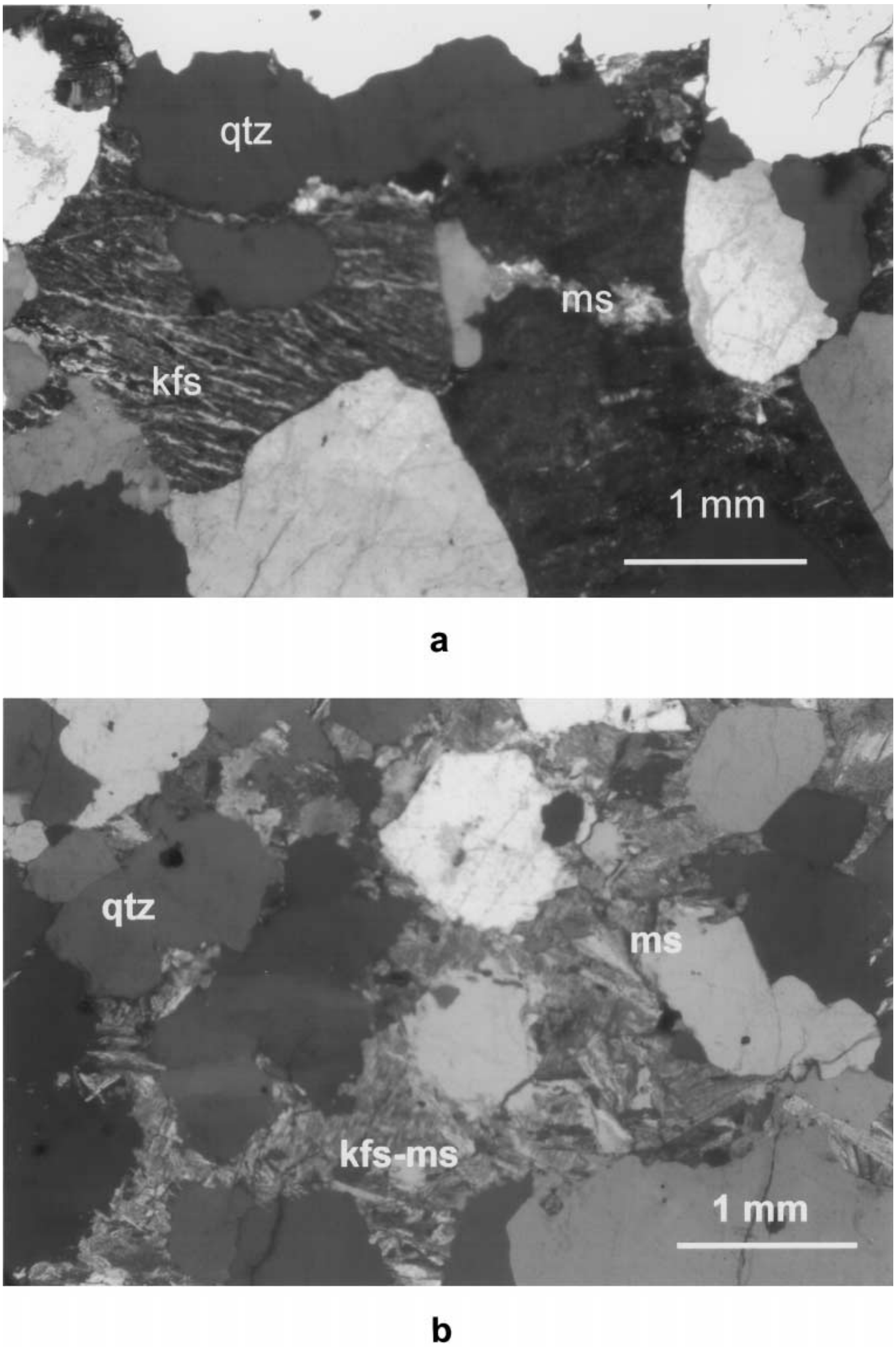

Fig. 7(a & b)—*Caption on p.* 1338.

Variation in granitoid textures outside the xenolith

If the xenolith had been descending through a magma similar in composition and texture to the regional porphyritic biotite monzogranite, it should have been surrounded by such material. We assume that the fine-grained aphyric material along the western contact, and the isotropic, leucocratic, equigranular, coarse-grained granitoid at the eastern end of the xenolith are significant and relevant to physical–chemical processes involving the xenolith.

Formation of the fine-grained rind at the western contact may be:

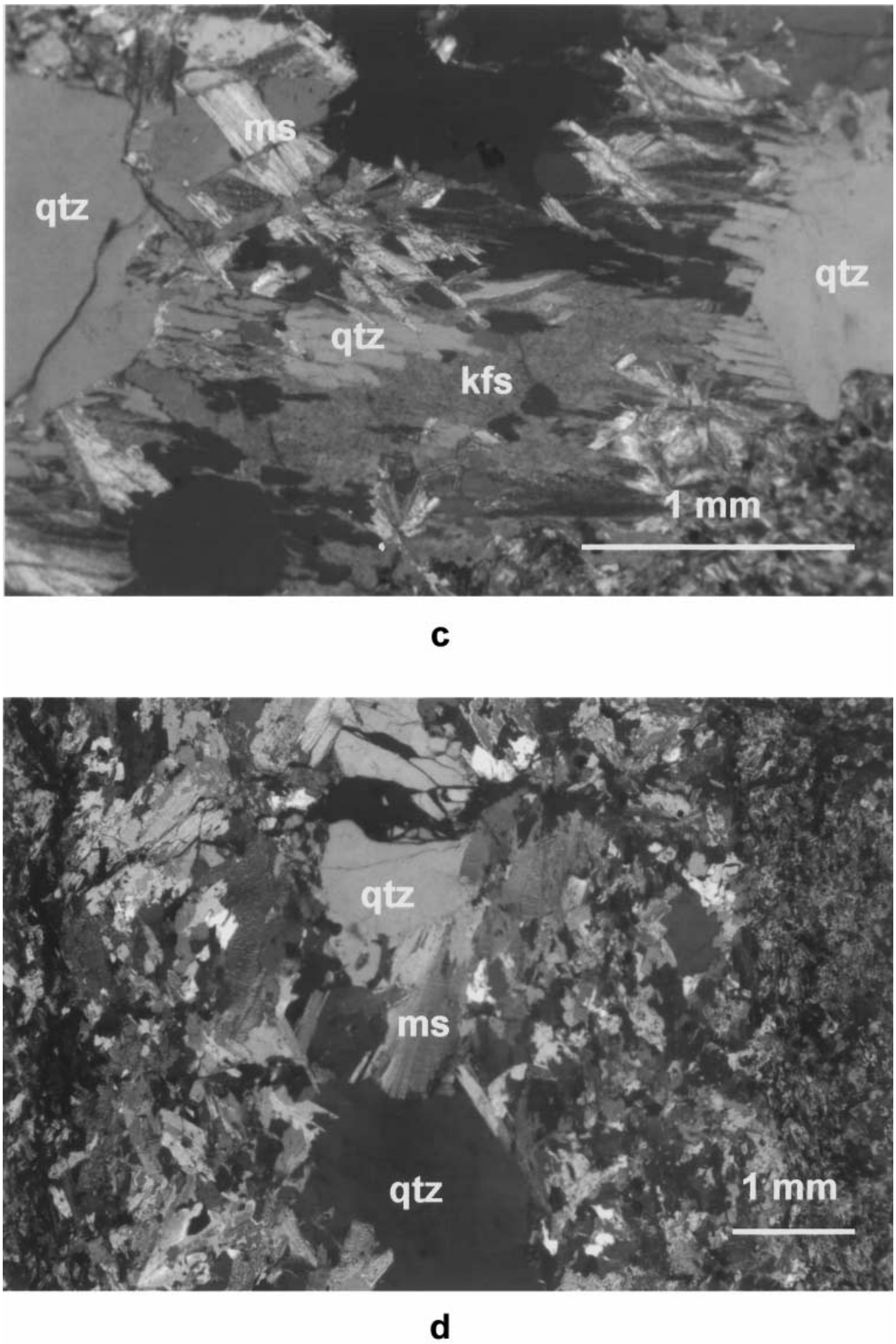

Fig. 7 (c & d)—*Caption overleaf.*

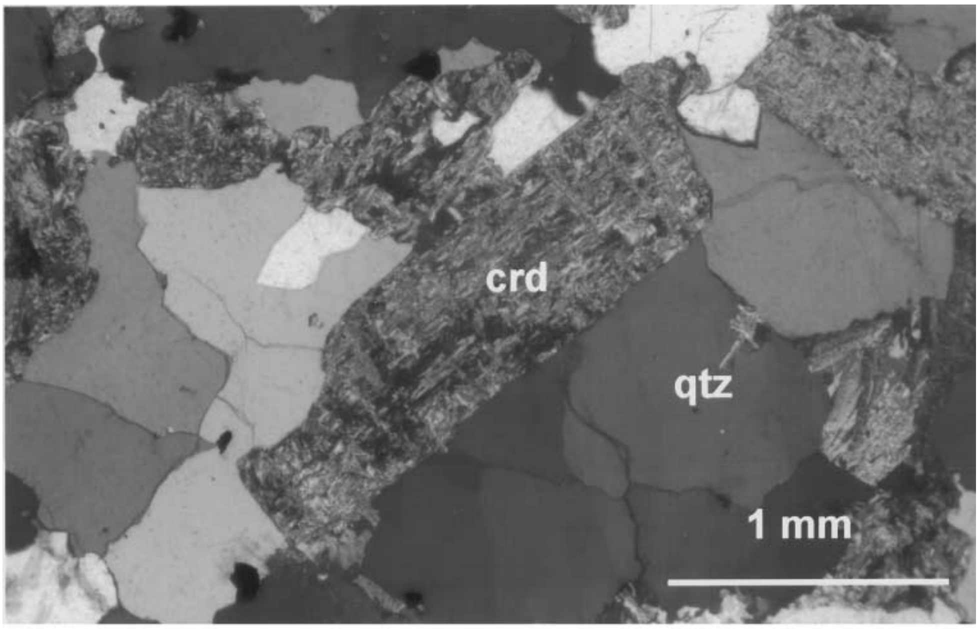

e

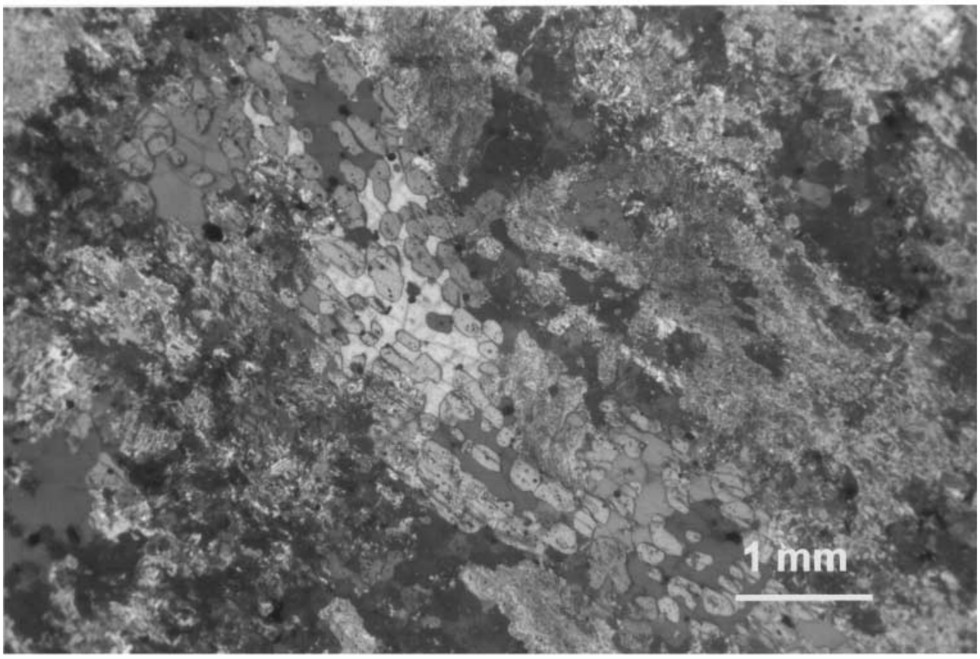

f

Fig. 7. Petrographic features of the granitoid rocks inside the fractured xenolith. (a) Sample PCX10 d, from a fracture 15 mm wide, showing typical granite texture. (b) Sample PCX10a, from a fracture 10 mm wide, showing euhedral to anhedral quartz grains in a continuous matrix of potassium feldspar and muscovite (cf. Fig. 6d). (c) Sample PCX10a, from a fracture 5 mm wide, showing a subhedral quartz grain on right side with comb-textured epitaxial overgrowths, and a lamellar intergrowth of quartz and potassium feldspar between the two quartz grains on the right and left sides of the field of view. Note also the radiating habit of the muscovites. (d) Sample PCX8a, a miniature aplite–pegmatite occupying a fracture 6 mm wide, showing symmetrically developed fine-grained margins flanking a relatively coarse-grained core of quartz and muscovite. (e) Sample PCX10a, from a fracture 10 mm wide, showing development of euhedral cordierite (now pinitized) in a quartz-rich matrix. (f) Sample PCX11a, from a discontinuous fracture, showing unusual development of aligned subhedral grains of anadalusite poikilitically enclosed in quartz.

Table 1. Parameters used in thermal modelling

Thermal parameter	Reference
$T_m^0 = 750°C$	estimated
$T_c^0 = 550°C$	estimated
$k_m = 4\ W\ m^{-1}\ K^{-1}$	Singer *et al.* (1989)
k_c(psammite) = $2\ W\ m^{-1}\ K^{-1}$	Guéguen and Palciauskas (1994) Touloukian *et al.* (1981)
k_c(pelite) = $2\ W\ m^{-1}\ K^{-1}$	Clauser and Huenges (1995)
$a_m = 1 \times 10^{-6}\ m^2\ s^{-1}$	Sakimoto and Zuber (1995)
a_c(psammite) = $6 \times 10^{-7}\ m^2\ s^{-1}$	Touloukian *et al.* (1981)
a_c(pelite) = $1 \times 10^{-6}\ m^2\ s^{-1}$	Guéguen and Palciauskas (1994) Touloukian *et al.* (1981) Clauser and Huenges (1995)
B(psammite) = 1×10^{10} Pa	Touloukian *et al.* (1981)
B(pelite) = 2×10^{10} Pa	Clark (1966)
α_v(psammite) = $3 \times 10^{-5}\ K^{-1}$	Touloukian *et al.* (1981)
α_a(pelite) = $6 \times 10^{-6}\ K^{-1}$	McKinstry (1965) Goldstein and Post (1969)
α_c(pelite) = $1.8 \times 10^{-5}\ K^{-1}$	McKinstry (1965) Goldstein and Post (1969)

(i) an aplitic quench, but the microscopic texture is unlike that of typical aplites in the area (Fig. 6c & d); or

(ii) a mechanical sorting of fine and coarse constituents—if rapid flow had taken place past this surface of the xenolith (an unusual variant of flowage differentiation in which the 'wall' moves relative to a static magma), the large K-feldspars would have migrated away from the region of high shear stresses leaving only the silicate melt and finer-grained material at this surface. A high concentration of K-feldspar phenocrysts does lie just beyond the fine-grained rind (Fig. 3c).

Although we currently have no further evidence to help in choosing between these alternatives, the second seems more likely.

In this part of the SMB, the porphyritic foliated biotite monzogranite is ubiquitous. The spatial relationship of the medium- to coarse-grained aphyric granitoid material to the east end of the xenolith suggests a genetic relationship with processes operating in the xenolith. Either this aphyric material represents magma that has passed right through the fractures, or it represents normal monzogranite magma to which an aqueous fluid phase that had occupied the tips of the propagating fractures has been added, or a combination of both. Even the pegmatite sheet that is in contact with the eastern end of the xenolith may owe its origin to such a fluid phase.

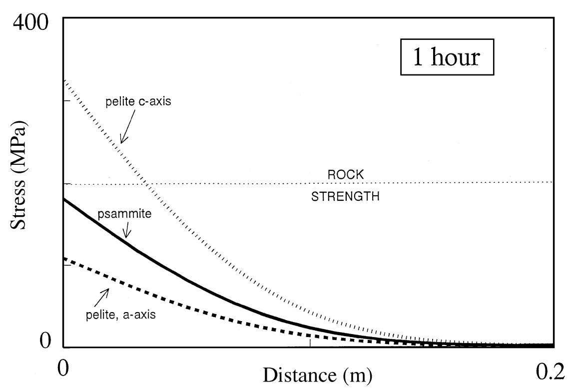

Fig. 8. Results of numerical modelling of thermal stress. The Portuguese Cove xenolith consists of isotropic psammite and anisotropic pelite. The curves on the diagram show the thermal stresses in these materials after 1 h of contact with the magma, as a function of distance from the contact with the granite magma. Stresses in the pelite, dominated by the *c*-axis direction in the muscovites, exceed rock strength to a distance of about 4 cm into the xenolith resulting in development of thermal stress fractures parallel to bedding.

Granitoid textures inside the xenolith. The most unusual textures of material filling the fractures are the miniature aplite–pegmatite systems, the ubiquitous muscovite sprays, the lamellar intergrowths of quartz and feldspar, and the quartz–andalusite intergrowths. The aplite–pegmatite and muscovite textures have well-established quench connotations. Rubin (1995) postulated that aplite–pegmatite systems originate in precisely this way: a normal water-undersaturated silicate melt becomes a quench aplite and a water-oversaturated pegmatite at the tip of the fracture (Fig. 9a). The comb–dendritic–lamellar intergrowths of quartz and feldspar, and the transition from euhedral to dendritic growth (Fig. 7c), appear to be characteristic of strong degrees of 'constitutional undercooling' (Lofgren and Donaldson, 1975; Swanson and Fenn, 1986). The quartz–andalusite intergrowths may be another, less familiar, manifestation of such oversaturation and rapid growth kinetics. We conclude that all these textures indicate rapid growth, probably under conditions of reduction in H_2O content of the silicate magma.

Final position of the stoped block

No clear answer to the question, "Why did the country rock stop where it did?" has come forward in the one hundred or so years since the recognition of magmatic stoping. The Stokes settling rate for a 25 m cube of country rock, with a density contrast of 300 kg m^{-3} between it and the granitoid magma, ranges from 0.1 m s^{-1} (for a magma viscosity of 10^6 Pa s) to 3.5 m s^{-1} (for a magma viscosity of 10^4 Pa s). At these rates, this block would require times between 14 h and 1.4 h to sink 5 km to the estimated floor (Garland, 1953) of the South Mountain Batholith. Three possible explanations for the current position of the Portuguese Cove xenolith are.

(i) It is a roof pendant—the attitude of the bedding in the xenolith is consistent with this interpretation, but at the current level of erosion, no way exists to know if this block had remained attached to its roof, although with all the documented fractures, attachment seems improbable, but nevertheless possible.

(ii) It detached very late into the highly viscous (Bingham rheology?) outer margin of the batholith—this interpretation is the standard explanation for the occurrence of large blocks in the

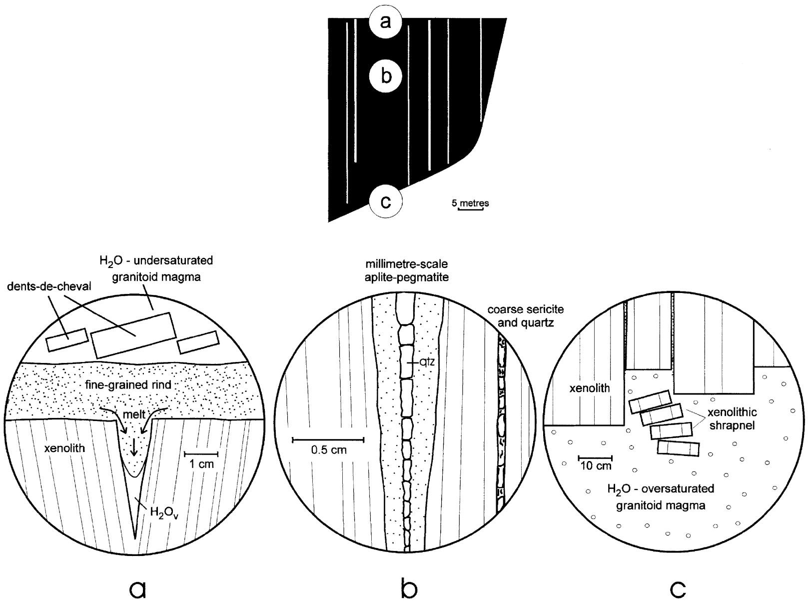

Fig. 9. Schematic representation of intrusion and disintegration processes. (a) Proximal or intake region showing the fine-grained rind, possibly the result of differential stresses and flowage differentiation in the melt at the margin of the sinking xenolith, and a rapidly propagating fracture led by water vapour and followed by silicate melt and fine-grained crystals. (b) Interior of the xenolith showing an aplite–pegmatite in which silicate melt and water-rich fluid have occupied the fracture, and a coarse sericite–quartz assemblage in which only water-rich fluid has occupied the fracture. (c) Distal end of the xenolith showing extensive fragmentation of the margin, possibly as the result of the emerging and expanding vapour phase.

margins of batholiths, and we have nothing further to add.

(iii) It is buoyed on a bubble of its own making—perhaps the release of an aqueous fluid phase, as evidenced by the aphyric material at the eastern end of the xenolith, was sufficient to suspend this particular xenolith, rather like a flotation cell for separating sulphides from silicates.

Physical consequences of disintegrating stoped blocks

For all his original and deep thinking about the stoping process, Daly never really addressed the question of elephants' graveyards. He simply believed that the stoped blocks were assimilated, i.e. "it seems legitimate to regard the abyssal portions of plutonic magmas as conspiring toward the perfect digestion of a foreign rock fragment" (Daly, 1903a, p. 288). However, rapid settling rates for large blocks leave little time for thermal contamination and no time for chemical assimilation, so elephants' graveyards should be an inevitable product of the piecemeal stoping process. We believe that the global evidence for the existence of stoping is inescapable, and that little evidence for elephants' graveyards exists. Thus, we conclude that stoped blocks must undergo *continuous* thermal stress fracturing and explosive exfoliation (or spalling) as they sink into the hotter regions of the magma, until no piece large enough to settle remains. In the extreme, this process of fragmentation could lead to the complete disintegration of the xenolith down to the level of individual grains, which then become xenocrysts.

Geochemical consequences of disintegrating stoped blocks

The xenolith at Portuguese Cove was clearly spalling debris into the surrounding granitic melt as it sank. The geochemical consequences of this combined stoping-plus-shattering process are manifest as greatly enhanced opportunities for assimilation of the stoped material (Furlong and Myers, 1985). Small refractory fragments, no longer able to sink, may then simply become xenoliths which may or may not react with the silicate melt. Small fusible fragments, also no longer able to sink, may undergo partial melting and hybridize with the main granite magma. Both of these cases of chemical assimilation cost the batholith thermal energy, whereas if thermal stress fragmentation reduces the xenoliths to individual xenocrysts, no further thermal energy is required for such mechanical assimilation.

Clarke *et al.* (1988) demonstrated that the $^{87}Sr/^{86}Sr_i$–εNd_i variation in the SMB with time was in the direction of the Meguma Group country rocks. Using just their isotopic ratios for early granodiorite (sample M72-137), late monzogranite (C-1, C-6, and C-16b), and weighted average Meguma Group, we estimate that the most evolved (contaminated) late monzogranites can be mixtures of as little as 60% early granodiorite with as much as 40% Meguma Group country rocks. We believe that such contaminated chemical compositions are the direct result of continuous mechanical disintegration and chemical assimilation of stoped blocks with time in the SMB. Such a scale of assimilation significantly increases the size of the pluton over the volume of granite magma introduced at the current level of exposure.

MODEL FOR DISINTEGRATION OF THE PORTUGUESE COVE XENOLITH

Field observations, particularly the high degree of fracturing of the original large xenolith, and the number of angular satellitic xenoliths adjacent to it, suggest intense and perhaps violent disintegration of the large xenolith. Petrographic observations of the material intruded into the large xenolith, particularly the variety of quench textures, suggest rapid crystallization. Thermal modelling shows that the anisotropic xenolith will develop thermal stress fractures quickly, and preferentially in the pelitic horizons.

Figure 9 shows three stages in the development of these fractures. When the thermal stress fracture forms, it represents a vacuum into which the magma will try to flow. Because elastic propagation rates for the fracture exceed viscous flow rates, the silicate melt will never be able to entirely fill the fracture (Rubin, 1993a). The high vacuum in the tip of the fracture will instantly draw dissolved water from the adjacent (normally water-undersaturated) silicate melt as a separate aqueous fluid phase (Fig. 9a). The chemical and physical properties of this fluid (weakening bonds and expanding volumetrically, respectively) greatly assisted fracture propagation. Depending on the width of the fracture and the distance from the intake surface, the fracture fill may be a miniature aplite (silicate-melt-rich fraction)–pegmatite (fluid-rich fraction), or even more distantly, a quartz–sericite hydrothermal vein (Fig. 9b). The fluid phase probably also permeated the xenolith causing extensive recrystallization of the sericite and alteration of the cordierite.

At the eastern contact, the emergence of the aqueous fluid phase may have contributed to the apparently explosive disintegration of the margin of the xenolith and the formation of xenolithic shrapnel (Fig. 9c).

Figure 10 summarizes the different types of thermal stress fracturing that could occur in unstrained xenoliths of three different types: (i) a homogeneous isotropic material in which only thermal gradient cracking can occur; (ii) a bi-material consisting of two isotropic

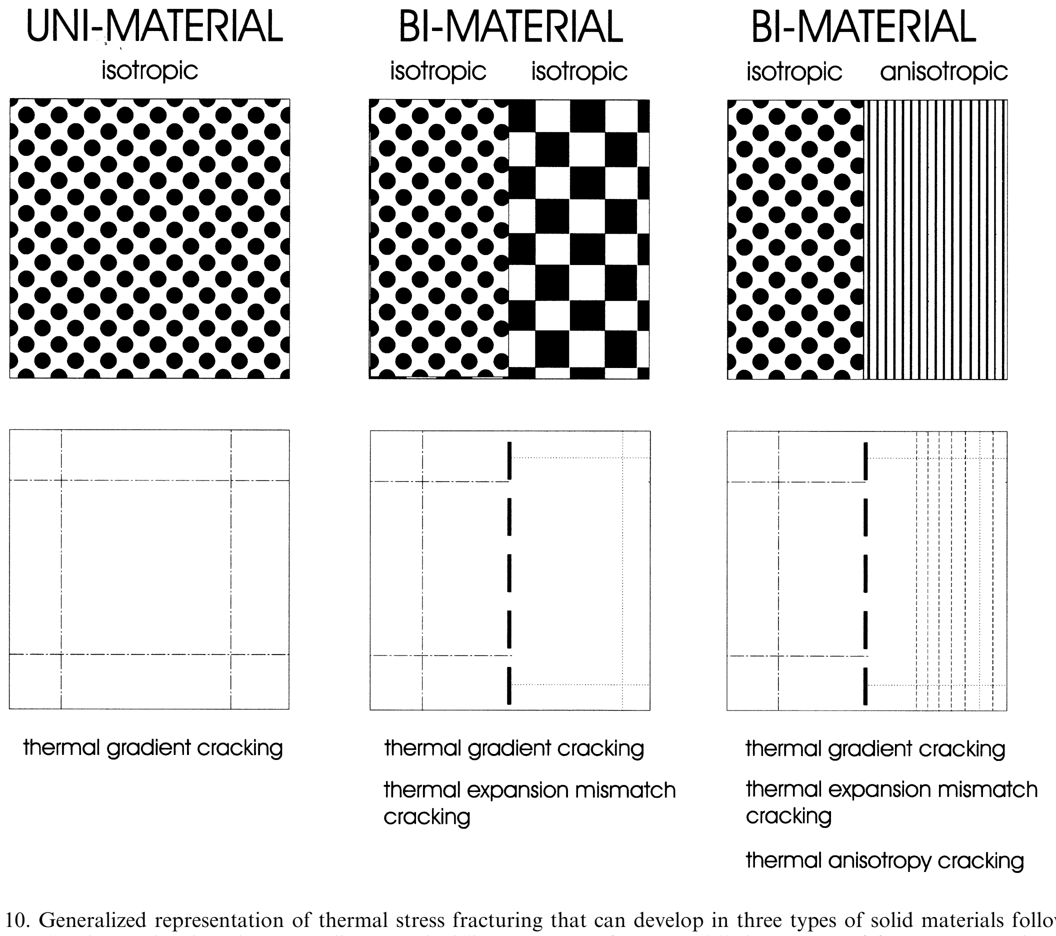

Fig. 10. Generalized representation of thermal stress fracturing that can develop in three types of solid materials following complete immersion in a hotter medium. Dashed lines represent fractures. All three types of fractures occur in the xenolith at Portuguese Cove: the cross-fractures are thermal gradient cracks, the fractures along the pelite–psammite contacts are thermal expansion mismatch cracks, and the fractures in the pelite are thermal anisotropy cracks.

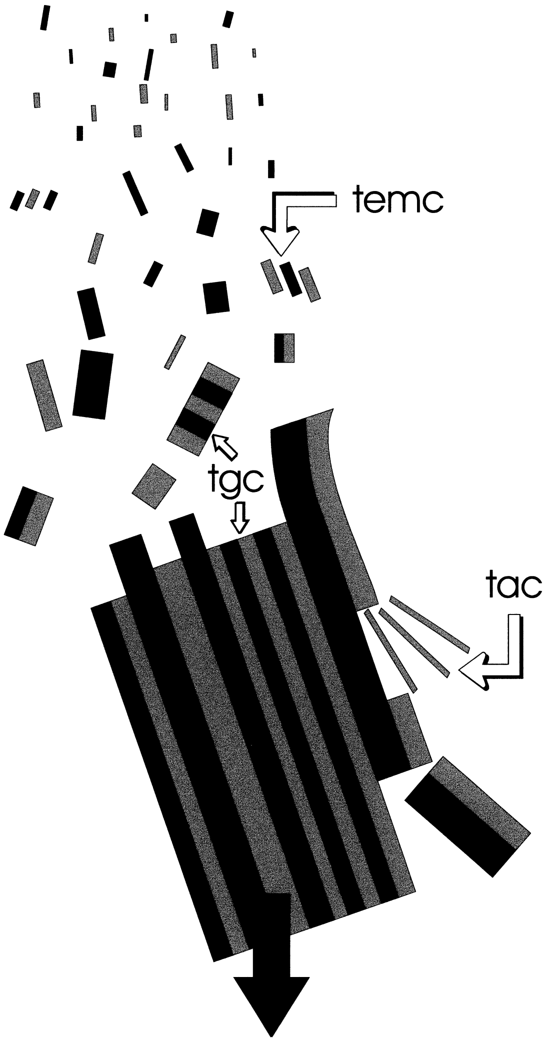

Fig. 11. Thermal stress fracturing and disintegration, independent of scale and material (see text). In the case of stoped blocks, the combined effects of thermal stress fracturing, unrelieved differential tectonic stresses, and explosive vapour release result in a continuous process of disintegration of the xenolith as it passes through the magma. All that remains of the stoped block is a wake of xenolithic shrapnel. (tac—thermal anisotropy crack; temc—thermal expansion mismatch crack; tgc—thermal gradient crack.)

materials in contact, in which thermal gradient cracking and thermal expansion mismatch cracking can occur; and (iii) a bi-material consisting of an isotropic material and an anisotropic material in contact, in which thermal gradient cracking, thermal expansion mismatch cracking, and thermal anisotropy cracking can all occur. The xenolith at Portuguese Cove shows evidence of thermal gradient cracking (the fractures at right angles to the bedding), thermal expansion mismatch cracking (granite sheets along the psammite–pelite contacts, Fig. 4), and thermal anisotropy cracking (granite sheets within the pelite horizons).

More generally, this process of break-up of the xenolith is similar to the initial slower disintegration of ice shelves in seawater (Parfit, 1997) or the faster fragmentation of meteorites in the atmosphere; in all these cases, cold solid material becomes immersed in a warmer medium, and thermal stress fracturing of the solid occurs. In the case of large stoped blocks, what remains is a wake of xenolithic debris in a disturbed granitic matrix, looking remarkably like xenolith-choked breccia pipes (Fig. 11).

CONCLUSIONS

Elephants' graveyards are the hypothetical final resting places for large blocks of country rock stoped from the roofs of batholiths. We believe that the apparent absence of such graveyards says more about the disintegration of stoped country rocks than the absence of stoping as a mechanism of ascent and emplacement. We have shown that thermal expansion of the country rock in contact with hot magma leads to thermal stresses in excess of rock strength in some directions after very short times, leading to anisotropic fracture preferentially in the pelitic materials. The same thermal stress fracturing that is responsible for stoping in the first place is also responsible for the disintegration of the stoped blocks as they descend through the magma chamber. The large country rock xenolith at Portuguese Cove preserves a state of arrested, or apprehended, disintegration. Under favourable thermal and structural conditions, stoped blocks will exfoliate, or even explode when a water-rich vapour phase appears, and the xenolithic shrapnel will become dispersed in the granite magma as a wake behind the descending stoped block. Those fragments may then undergo mechanical disaggregation and chemical assimilation to the point that they are no longer *physically* recognizable. All that remains of the stoping process is a component of *chemical* variation toward the composition of the wallrocks. The isotopic variation in the South Mountain Batholith shows such progressive interaction with country rock material.

Acknowledgements—The Department of Earth Sciences at Dalhousie University is grateful to the Wolfe family for permitting a generation of Dalhousie University earth science students to access their property to observe the 'big xenolith'. We would like to thank Basil Cooke and Clint Milligan for introducing us to this outcrop many years ago, as well as Nick Culshaw, Becky Jamieson, Gail Mahood, and a class of graduate students who acted as valuable sounding boards for our ideas. Bernard Bonin, John Clemens, Ken McCaffrey, Clint Milligan, Matt Slagel, and Aaron Yoshinobu generously offered comments on a draft version of this paper, and Keith Benn, Kevin Furlong, and Nick Petford provided constructive suggestions for improvement in their reviews. We also wish to thank Michael MacDonald of the Nova Scotia Department of Natural Resources for the excellent airphoto on which we based our detailed map, and Paul Hill of Dalhousie University for valuable consultations on sinking rates of stoped blocks. Jane Anne Horne and Lynne Maillet-Frotten generously made the digital photomicrographs possible. We also acknowledge the Natural Sciences and Engineering Research Council of Canada (NSERC) for supporting the research of DBC and MAW. MAW also acknowledges the contribution of the Killam Trusts.

REFERENCES

Abbott, R. N. (1989) Internal structures in part of the South Mountain Batholith, Nova Scotia, Canada. *Geological Society of America Bulletin* **101,** 1493–1506.

Balk, R. (1937) Structural behaviour of igneous rocks. *Geological Society of America Memoir* **5,** 177 pp.

Benn, K., Horne, R. J., Kontak, D. J., Pignotta, G. S. and Evans, N. G. (1997) Syn-Acadian emplacement model for the South Mountain batholith, Meguma Terrane, Nova Scotia: Magnetic fabric and structural analyses. *Geological Society of America Bulletin* **109,** 1279–1293.

Buddington, A. F. (1959) Granite emplacement with special reference to North America. *Geological Society of America Bulletin* **70,** 671–747.

Carslaw, H. S. and Jaeger, J. C. (1959) *Conduction of Heat in Solids*. Oxford University Press, Oxford.

Castro, A. (1987) On granitoid emplacement and related structures. A review. *Geologische Rundschau* **76/1,** 101–124.

Clark, S. P., Jr (editor) (1966) Handbook of Physical Constants. Geological Society of America Memoir, **97**.

Clarke, D. B. and Muecke, G. K. (1985) Review of the petrochemistry and origin of the South Mountain Batholith and associated plutons. In *High Heat Production (HHP) Granites, Hydrothermal Circulation, and Ore Genesis*, pp. 41–54. The Institute of Mining and Metallurgy, London.

Clarke, D. B., Halliday, A. N. and Hamilton, P. J. (1988) Neodymium and strontium isotopic constraints on the origin of the peraluminous granitoids of the South Mountain Batholith, Nova Scotia, Canada. *Chemical Geology (Isotope Geoscience Section)* **73,** 15–24.

Clarke, D. B., MacDonald, M. A., Reynolds, P. H. and Longstaffe, F. J. (1993) Leucogranites from the eastern part of the South Mountain Batholith, Nova Scotia. *Journal of Petrology* **34,** 653–679.

Clauser, C. and Huenges, E. (1995) Thermal conductivity of rocks and minerals. *Thermal Conductivity* **5,** 103–126.

Clemens, J. D. and Mawer, C. K. (1992) Granitic magma transport by fracture propagation. *Tectonophysics* **204,** 339–360.

Cooke, H. B. and Milligan, G. C. (1980) *Trip 11: Magmatic Stoping at Meguma–Granite Contact near Halifax, Nova Scotia*. Geological Association of Canada—Mineralogical Association of Canada Field Trip Guidebook.

Daly, R. A. (1903a) The mechanics of igneous intrusion. *American Journal of Science* **15,** 269–298.

Daly, R. A. (1903b) The mechanics of igneous intrusion (Second Paper). *American Journal of Science* **16,** 107–126.

Daly, R. A. (1933) *Igneous Rocks and the Depths of the Earth*. McGraw-Hill, New York.

Fowler, T. K. and Paterson, S. R. (1997) Timing and nature of magmatic fabrics from structural relations around stoped blocks. *Journal of Structural Geology* **19,** 209–224.

Furlong, K. P. and Myers, J. D. (1985) Thermal–mechanical modelling of the role of thermal stresses and stoping in magma contamination. *Journal of Volcanology and Geothermal Research* **24,** 179–191.

Garland, G. D. (1953) Gravity measurements in the Maritime Provinces. *Dominion Observatory of Canada* **16,** 185–275.

Glenn, L. A., Gommerstadt, B. Y. and Chudnovsky, A. (1986) A fracture mechanics model of fragmentation. *Journal of Applied Physics* **60,** 1224–1226.

Goldstein, L. and Post, B. (1969) Thermal expansion coefficients of ruby muscovite mica. *Journal of Applied Physics* **40,** 3056–3057.

Goodchild, J. G. (1892) Note on a granite junction in the Ross of Mull. *Geological Magazine* **9,** 447–451.

Goodchild, J. G. (1894) Augen-structure in relation to the origin of the eruptive rocks and gneiss. *Geological Magazine* **1,** 20–27.

Grady, D. E. and Kipp, M. E. (1985) Mechanisms of dynamic fragmentation: factors governing fragment size. *Mechanics of Materials* **4,** 311–320.

Guéguen, Y. and Palciauskas, V. (1994) *Introduction to the Physics of Rocks*. Princeton University Press, Princeton.

Ivanov, A. G., Raevskii, V. A. and Vorontsova, O. S. (1995) Explosive fragmentation of materials. *Combustion, Explosion and Shock Waves* **31,** 211–215.

Lister, J. R. and Kerr, R. C. (1991) Fluid–mechanical models of crack propagation and their application to magma transport in dykes. *Journal of Geophysical Research* **96,** 10,049–10,077.

Lofgren, G. E. and Donaldson, C. H. (1975) Curved branching crystals and differentiation in comb-layered rocks. *Contributions to Mineralogy and Petrology* **49,** 309–319.

MacDonald, M. A., Corey, M. C., Ham, L. J. and Horne, R. J. (1992) An overview of recent bedrock mapping and follow-up petrological studies of the South Mountain Batholith, southwestern Nova Scotia, Canada. *Atlantic Geology* **28,** 7–28.

MacDonald, M. A. and Horne, R. J. (1987) *Bedrock Geological Map of Halifax and Sambro NTS sheets 11D/12 and part of 11D/05*. Nova Scotia Department of Mines and Energy, Map 87-6, scale 1:50,000.

MacDonald, M. A. and Horne, R. J. (1988) Petrology of the zoned, peraluminous Halifax pluton, south-central Nova Scotia. *Maritime Sediments and Atlantic Geology* **24,** 33–46.

Marsh, B. D. (1982) On the mechanics of igneous diapirism, stoping, and zone melting. *American Journal of Science* **282,** 808–855.

McKinstry, H. A. (1965) Thermal expansion of clay minerals. *American Mineralogist* **50,** 212–222.

Michalske, T. A. and Bunker, B. C. (1987) The fracturing of glass. *Scientific American* **257,** 122–129.

Parfit, M. (1997) A dream called Nunavut. *National Geographic* **192,** 68–91.

Paterson, S. R., Fowler, T. K. and Miller, R. B. (1996) Pluton emplacement in arcs: a crustal exchange process. *Transactions of the Royal Society of Edinburgh: Earth Sciences* **87,** 115–123.

Pitcher, W. S. (1993) *The Nature and Origin of Granite*. Blackie Academic and Professional, London.

Rauenzahn, R. M. and Tester, J. W. (1989) Rock failure mechanisms of flame-jet thermal spallation drilling—theory and experimental testing. *International Journal of Rock Mechanics and Mining Sciences Geomechanics Abstracts* **26,** 381–399.

Read, H. H. (1948) Granites and granites. In *Origin of Granite*. ed. J. Gilluly. Geological Society of America Memoirs. **28,** pp. 1–19.

Rubin, A. M. (1993a) Tensile fracture of rock at high confining pressure: implications for dike propagation. *Journal of Geophysical Research* **98,** 15919–15935.

Rubin, A. M. (1993b) Dikes vs. diapirs in viscoeleastic rock. *Earth and Planetary Science Letters* **117,** 653–670.

Rubin, A. M. (1995) Getting granite dikes out of the source region. *Journal of Geophysical Research* **100,** 5911–5929.

Sakimoto, S. E. H. and Zuber, M. T. (1995) Effects of planetary thermal structure on the ascent and cooling of magma on Venus. *Journal of Volcanology and Geothermal Research* **64,** 53–60.

Schenk, P. E. (1991) Events and sea-level changes on Gondwana's margin: the Meguma Zone (Cambrian–Devonian) of Nova Scotia, Canada. *Geological Society of America Bulletin* **103,** 512–521.

Singer, B. S., Myers, J. D., Linneman, S. R. and Angeveine, C. L. (1989) The thermal history of ascending magma diapirs and the thermal and physical evolution of magmatic conduits. *Journal of Volcanology and Geothermal Research* **37,** 273–289.

Spence, D. A. and Turcotte, D. L. (1985) Magma-driven propagation of cracks. *Journal of Geophysical Research* **90,** 575–580.

Sugioka, I. and Bursik, M. (1995) Explosive fragmentation of erupting magma. *Nature* **373,** 689–692.

Swanson, S. E. and Fenn, P. M. (1986) Quartz crystallization in igneous rocks. *American Mineralogist* **71,** 331–342.

Tardif, H. P. and Sterling, T. S. (1967) Explosively produced fractures and fragments in forensic investigations. *Journal of Forensic Sciences* **12,** 247–272.

Tate, M. C. (1994) The nature and origin of enclaves in four peraluminous granitoid intrusions from the Meguma Zone, Nova Scotia. *Atlantic Geology* **30,** 205–215.

Touloukian Y. S., Judd, W. R. and Roy, R. F. (eds) (1981) *Physical Properties of Rocks and Minerals*. McGraw-Hill, New York.

Williams, H. and Hatcher, R. D. (1982) Suspect terranes and the accretionary history of the Appalachian orogen. *Geology* **10,** 530–536.